High-order harmonic generation directly from a filament

2011 New J. Phys. 13 043022

(http://iopscience.iop.org/1367-2630/13/4/043022)

New Journal of Physics
The open-access journal for physics

High-order harmonic generation directly from a filament

D S Steingrube[1,2,8], E Schulz[1,2], T Binhammer[3], M B Gaarde[4,5], A Couairon[6], U Morgner[1,2,7] and M Kovačev[1,2]

[1] Leibniz Universität Hannover, Institut für Quantenoptik, Welfengarten 1, D-30167 Hannover, Germany
[2] QUEST, Centre for Quantum Engineering and Space-Time Research, Hannover, Germany
[3] VENTEON Laser Technologies GmbH, D-30827 Garbsen, Germany
[4] Department of Physics and Astronomy, Louisiana State University, Baton Rouge, LA 70803-4001, USA
[5] PULSE Institute, SLAC National Accelerator Laboratory, Menlo Park, CA 94025, USA
[6] Centre de Physique Théorique, École Polytechnique, CNRS, F-91128, Palaiseau, France
[7] Laser Zentrum Hannover e.V., Germany
E-mail: steingrube@iqo.uni-hannover.de

New Journal of Physics **13** (2011) 043022 (11pp)
Received 17 December 2010
Published 15 April 2011
Online at http://www.njp.org/
doi:10.1088/1367-2630/13/4/043022

Abstract. The synthesis of isolated attosecond pulses (IAPs) in the extreme ultraviolet (XUV) spectral region has opened up the shortest time scales for time-resolved studies. It relies on the generation of high-order harmonics (HHG) from high-power few-cycle infrared (IR) laser pulses. Here we explore experimentally a new and simple route to IAP generation directly from 35 fs IR pulses that undergo filamentation in argon. Spectral broadening, self-shortening of the IR pulse and HHG are realized in a single stage, reducing the cost and experimental effort for easier spreading of attosecond sources. We observe continuous XUV spectra supporting IAPs, emerging directly from the filament via a truncating pinhole to vacuum. The extremely short absorption length of the XUV radiation makes it a highly local probe for studying the elusive filamentation dynamics and in particular provides an experimental diagnostic of short-lived spikes in

[8] Author to whom any correspondence should be addressed.

laser intensity. The excellent agreement with numerical simulations suggests the formation of a single-cycle pulse in the filament.

Contents

1. Introduction

Attosecond science is now a mature field of modern physics, as demonstrated through a range of both time-resolved and spectroscopic applications [1]–[6]. The key strong-field process allowing for the synthesis of isolated attosecond pulses (IAPs) requires that high-intensity ultra-short infrared (IR) laser pulses, ideally with near single-cycle durations, interact with a noble gas, leading to a continuous extreme ultraviolet (XUV) spectrum via high-order harmonic generation (HHG) [3], [7]–[9]. So far, few-cycle driving pulses exploited for attosecond pulse synthesis are produced by gating methods [10]–[14], or by spectral broadening in hollow core fibers [15]–[18] usually followed by recompression with chirped mirrors, and transported to a low-pressure gas medium for HHG [19]. Direct ionization-induced self-compression of a laser pulse propagating in a hollow waveguide filled with a low-pressure argon gas was also exploited and shown to be advantageous for extending high harmonic emission to very high photon energies [16, 20, 21]. In the absence of any external guiding mechanism, phase-matched generation of high-order harmonics was optimized with long focus geometries leading to an interaction over 10–15 cm in low-pressure (typically 2 torr) argon or xenon gas cells [22, 23].

Filamentation constitutes an alternative method for the generation of ultra-short driver pulses [24]–[26], with peculiar features including extreme simplicity and energy up-scalability, both being invaluable advantages for ultra-fast, strong-field applications. Filamentation exhibits a significantly different physics from standard interaction schemes in low-pressure gases. A distinguishing feature of filaments is the prevailing role of beam self-focusing and collapse occurring when the pulse peak power exceeds a critical threshold $P_{cr} = 3.77\lambda^2/8\pi n_0 n_2$, where n_2 is the nonlinear Kerr index coefficient of the medium. In a gas at atmospheric pressure, the critical power is a few GW, whereas at 10^{-3} bar it reaches the TW level, leading to the property that a filament cannot be observed below a certain pressure that depends on the available pulse energy. When the peak power of a multicycle laser pulse exceeds the critical threshold, filamentation takes place as a spontaneous dynamical reshaping of the pulse in both time and space [27, 28]. This leads to self-shortening in time, and self-narrowing in space, so that the beam forms a hot core that is surrounded by a low-intensity energy reservoir. The laser propagation in the filament is self-sustained over an extended distance due to a net inward energy

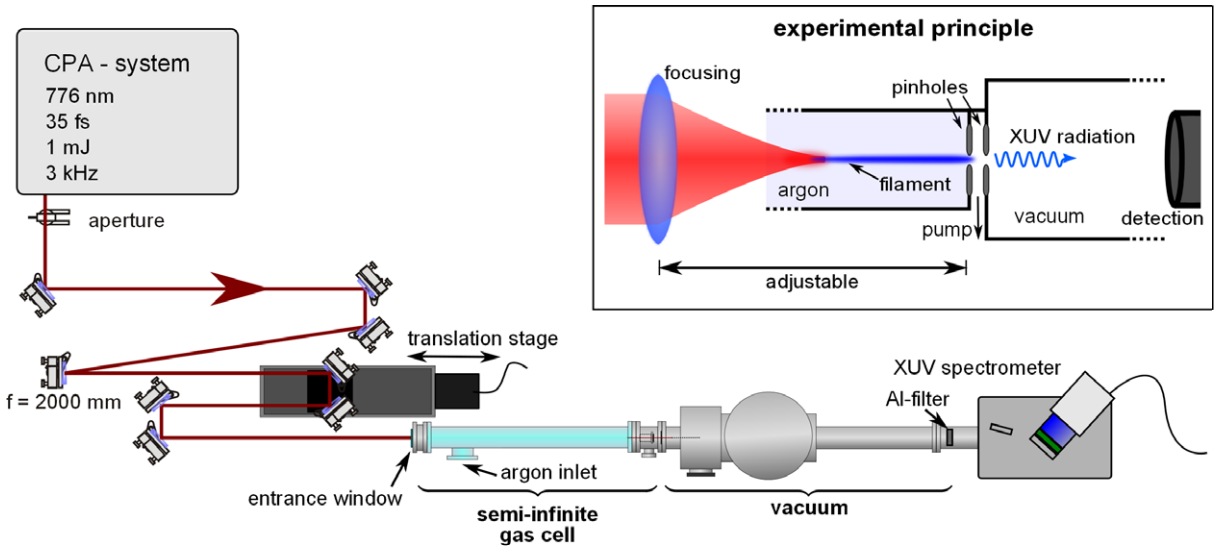

Figure 1. Experimental setup. A filament is generated by loosely focusing the laser beam into a semi-infinite gas cell filled with argon. At an abrupt transition to vacuum, high-order harmonic radiation in the XUV spectral region is extracted and monitored along the filament by changing the distance between the focusing optics and the pinhole.

flux from the reservoir to the core [29, 30]. This occurs at certain positions within a filament, resulting in the formation of spatiotemporal intensity spikes that can reach the single-cycle limit. These can in turn be exploited as driver pulses for HHG [31, 32].

In this paper, we report on HHG directly inside a filament, with a bandwidth that supports the generation of isolated attosecond XUV pulses. By introducing a steep transition from gas to vacuum, the filament is truncated while the generated harmonic radiation is extracted. A detailed analysis of the harmonic beam reveals a homogeneous spatial profile and conversion efficiencies comparable to traditional gas targets. Using this radiation as a probe, we demonstrate a unique tool for the investigation of the complex dynamics within a filament. Numerical calculations are in excellent agreement with the experiment and reveal that the high intensity spikes lead to the observed continuous harmonic spectra and can produce IAPs.

2. Experimental setup

In our experiment, sketched in figure 1, a commercial titanium–sapphire amplifier system (Dragon, KMLabs Inc.) delivers 35 fs pulses with a central wavelength of 780 nm and 1 mJ pulse energy at 3 kHz repetition rate. An aperture of 7.5 mm diameter transmits 80% of the pulse energy, which yields about 21 GW peak power and 4.1 times the critical power for self-focusing in 1 atm argon, estimated with the nonlinear index coefficient $n_2 = 1.74 \times 10^{-19}\,\mathrm{cm^2\,W^{-1}}$. With a focusing mirror of 2 m focal length a filament is generated in a 1 m long semi-infinite gas cell (SIGC) [33, 34] filled with argon at atmospheric pressure. A laser-drilled pinhole in a metal plate (diameter: 500–800 μm) truncates the filament abruptly by terminating the high-pressure cell. Behind a second laser-drilled pinhole (diameter: about 250 μm) placed 1 cm distance from the first one, the background pressure is below 5×10^{-4} mbar. The phase-matching at 1 atm of

argon is dominated by absorption. The absorption length at 1 atm is 10 μm for 20 eV radiation, and 50 μm for 38 eV, which is the high end of the observed harmonic spectra. In that sense, the harmonic output is a measure of only the last few tens of microns of propagation before the first pinhole, where it is transmitted into vacuum and propagates with low absorption to an XUV spectrometer. By changing the distance between the focusing optics and the truncation pinhole, we translate the truncation across the length of the filament, thereby scanning the HHG origin as a function of the filament length. The distance is changed by a motorized translation stage placed between the focusing mirror and the 2 mm CaF_2 entrance window of the SIGC. The transmitted harmonics act as a highly nonlinear probe for systematic investigations of local intensity [35, 36] and pulse duration [31, 32]. After filtering by a 200 nm thick aluminum foil at 1 m distance from the pinholes, the harmonic radiation is recorded by using two XUV spectrometers (LHT 30, Horiba-Jobin-Yvon with 500 lines mm^{-1}; 248/310-G, McPherson, with 300 lines mm^{-1} and CCD DH420A-F0, ANDOR Technology).

3. Numerical methods

We solve the coupled Maxwell wave equation and the time-dependent Schrödinger equation in a formulation that has sub-cycle time resolution. The wave equation is transformed into a uni-directional propagation equation, which is first order in the propagation coordinate and is solved via space-marching in the frequency domain, for all frequencies comprising the laser and harmonic spectra; see [32, 37] for details. For each plane in the propagation direction, we find the time-dependent laser electric field via inverse transform of its spectrum and use it to calculate the (time-dependent) nonlinear source terms, as described below. We then Fourier transform the source terms back to the frequency domain and use them to propagate the laser and harmonic frequencies to the next plane in the propagation direction. For the laser field, the nonlinear terms include the third-order response described by the third-order susceptibility $\chi^{(3)}$, and the ionization driven terms that are evaluated using intensity-dependent ionization rates calculated, as described in [38]. The ionization terms are the nonlinear absorption via multiphoton ionization, and the ionization-driven plasma refractive index. For the harmonic field the source term is given by the time-dependent dipole moment, calculated using the strong field approximation [39], multiplied by the atomic density. Absorption (for frequencies above the ionization threshold) and linear dispersion are treated with frequency-dependent coefficients taken from [40, 41].

4. High-order harmonic generation (HHG) directly from a filament

In the experiment, we measure high-order harmonic spectra at different positions of the truncating pinhole in the filament. In figure 2(a), we identify two regions where harmonics are produced with high yield. The region around 211 cm from the focusing optics exhibits a resolved harmonic structure, whereas the second region around 219 cm shows a continuous spectral shape. The harmonic profiles, shown at the top of figure 2(a), are measured in the far field 1.5 m from the pinholes for harmonics in the resolved as well as in the continuous region. In both regions a Gaussian beam is observed, showing the applicability of the harmonic radiation as well as the good quality of the fundamental pulse in the filament generating the harmonics. The best conversion efficiency is measured as 1.3×10^{-7} for the harmonic radiation in the range from 30 to 50 nm via an XUV diode (AXUV100, International Radiation Detectors,

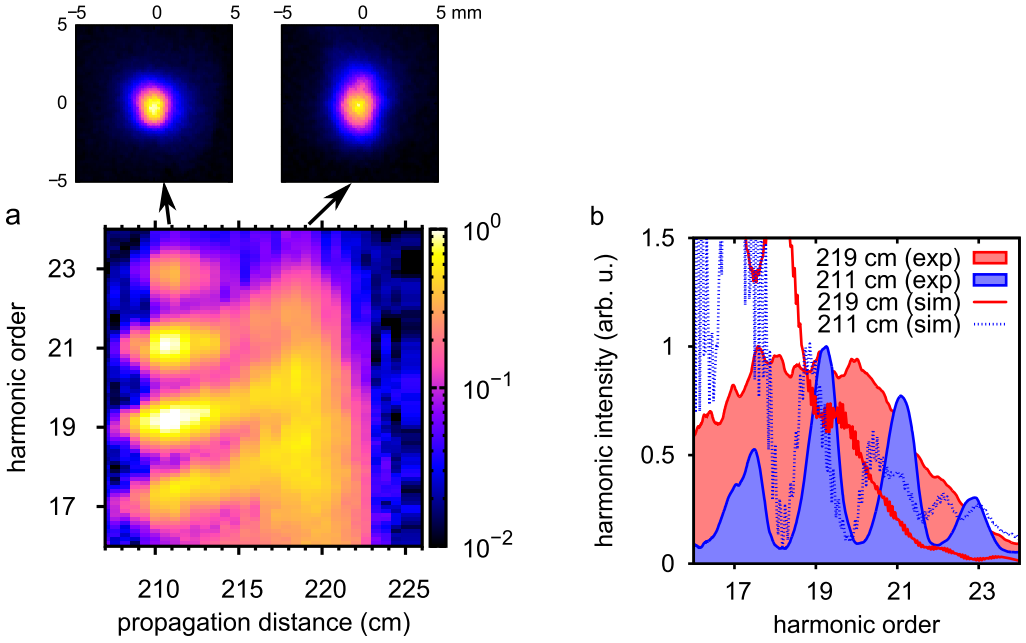

Figure 2. Experimental HHG from a filament. (a) Map of the high-order harmonic yield versus order and propagation distance recorded along the filament. The measurements reveal one area of resolved and one area of continuous harmonic distribution. The spatial profiles of the harmonic beam measured in the far field at the corresponding positions of extraction are shown at the top of the graph. (b) Harmonic spectra from panel (a) at selected positions in the resolved and continuous region. For comparison, simulated on-axis spectra are shown as dashed curves.

Inc.) with a flat response of $0.25\,\mathrm{A\,W^{-1}}$ in this range after three aluminum filters of 300 nm thickness each. At pinhole positions smaller than 207 cm or larger than 223 cm, no significant harmonic contribution is observed, even though the fluorescence of the filament expands over 25–30 cm. Figure 2(b) shows harmonic spectra at the two major regions on a linear scale. The highest harmonic order of 23 and the cutoff law [42] scaling as $I\lambda^2$ allows for the estimation of a lower bound for the driving laser intensity to $1.2 \times 10^{14}\,\mathrm{W\,cm^{-2}}$, assuming a non-chirped driving pulse with $\lambda = 780$ nm. As the carrier–envelope phase (CEP) of our laser system is not stabilized, single-shot spectra were taken at selected positions by gating the multichannel plate of our spectrometer. The continuous feature of the spectrum at 219 cm is preserved from shot to shot extending to similar cutoffs (see figure 3). We note that whereas the measured spectra represent essentially only the on-axis part of the beam in the horizontal direction, they are spatially averaged in the vertical direction due to the dimensions of the spectrometer entrance slit. We therefore cannot exclude that the smooth spectrum is a result of spatial averaging. However, as discussed below, our calculations indicate that the harmonic spectrum driven by this intensity spike is continuous both on-axis and off-axis.

The experimentally measured harmonic spectra stem from the complex spatiotemporal dynamics of the driving laser pulse in the filament. A recent theoretical work predicts the repeated occurrence of ultra-fast intensity spikes by the formation of intense sub-pulses with single optical cycle duration and peak intensities exceeding the equilibrium intensity by more

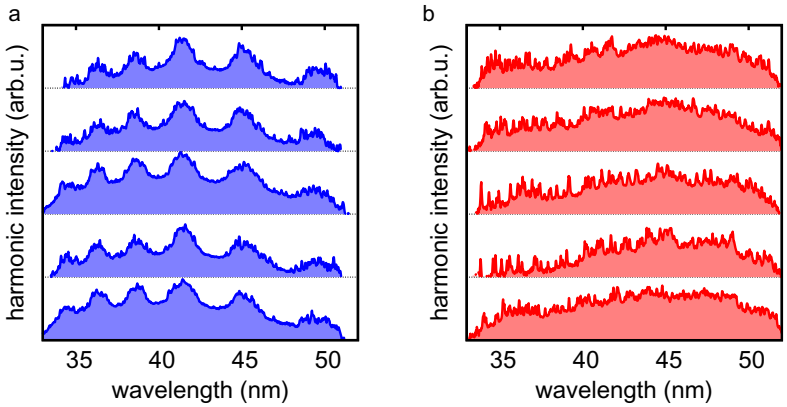

Figure 3. Single-shot spectra. Measured single-shot spectra on a logarithmic scale showing (a) resolved harmonics around 211 cm and (b) a continuous structure around 219 cm.

than a factor of three [32]. A spike is formed when the trailing edge of the pulse, which has been defocused due to strong ionization in the beam center, becomes refocused onto the axis at distances too short to preserve the equilibrium between the inward energy flux and nonlinear absorption. The intense sub-pulse propagates 1–2 cm before it undergoes another defocusing–refocusing cycle. The graph of figure 4(a) displays the calculated on-axis IR intensity along the filament with three spikes. HHG constitutes a signature of the presence of intensity spikes. Our experimental spectra reveal the first intensity spike around 211 cm, generating well-resolved harmonics which corresponds to a driving pulse of several cycles. The observation of a continuous harmonic spectrum around 219 cm suggests that the second spike occurs with an even shorter pulse duration. We note that the filament itself is much longer than the region over which we produce harmonics. This means that our experiment clearly reveals an important characteristic of the filament: (i) the peak intensity increases substantially at several distances along the propagation axis, of direct interest to filament applications that require high peak intensities. This observation further suggests (ii) the presence of an energy flux from the cold periphery of the beam toward the intense core of the filament, often conjectured but rarely simulated or measured in a gas filament so far [43, 44]. Intensity spikes obtained at specific positions are a direct signature of this energy flux. The observation of one region with spectrally resolved harmonics and one region with a continuous spectrum finally suggests that (iii) the self-compression process reaches beyond the few-cycle limit to the near-single-cycle limit. All of these observations are strongly supported by the numerical results.

5. Numerical results

Our interpretation of the experimental spectra is confirmed by the excellent agreement between the measurements in figure 2 and calculated harmonic spectra shown in figure 4. We performed large-scale numerical calculations with sub-optical-cycle precision, including both the filamentation dynamics and the generated harmonic radiation [32, 37]. The calculation starts at the beginning of the 1 atm argon gas cell with a 35 fs, 800 nm laser pulse of a peak intensity of approximately 10^{12} W cm^{-2} mimicking the experimental conditions. To account for

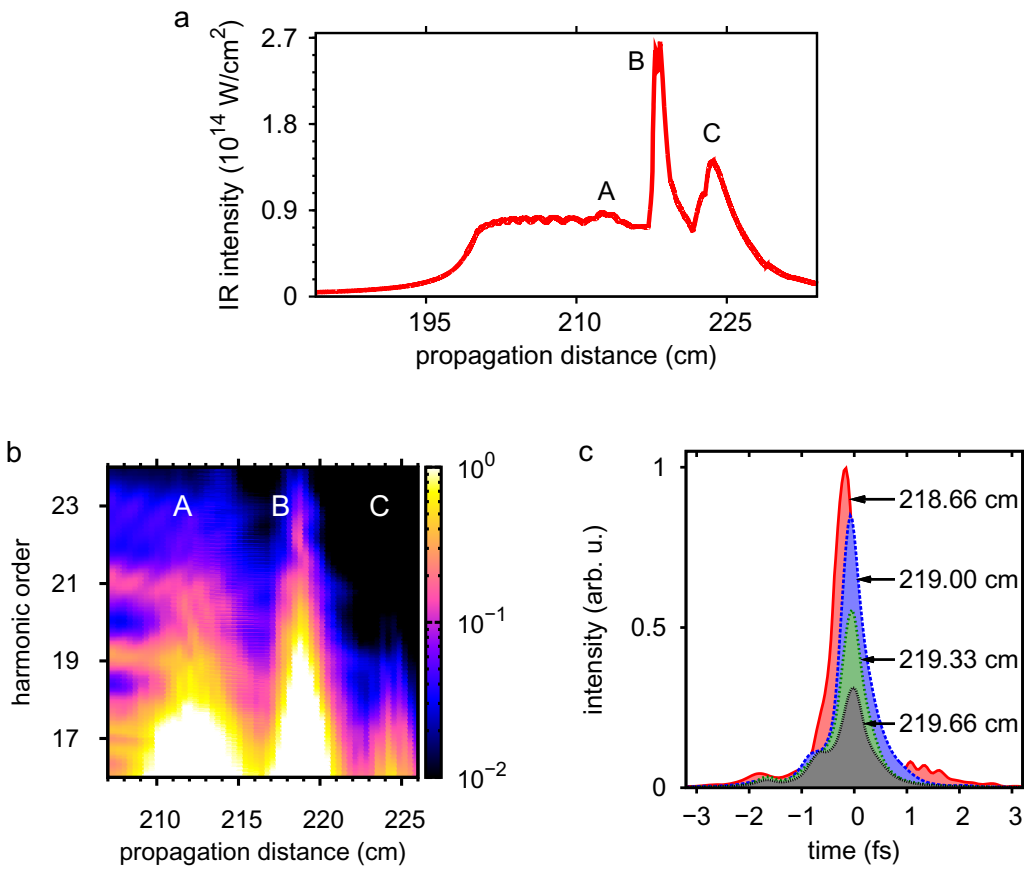

Figure 4. Simulated HHG from a filament. (a) Simulated intensity evolution of the IR field in the filament with the occurrence of intensity spikes (A, B, C). (b) Calculated high-order harmonic spectra from a filament generated at different positions in the filament. The simulation was performed in conditions comparable to the experiment. (c) Time profile of the single-attosecond pulses extracted at different positions within the filament.

intensity and phase fluctuations in the experiment, we have averaged over a few different values of the laser CEP (zero and π) and peak intensity ($\pm$5–10% of the peak intensity). We have also multiplied with a spectral filter simulating the spectral response of the aluminum foil and the detector.

Figure 4(a) shows the laser peak intensity versus propagation distance for this filament and figure 4(b) its resulting harmonic spectrum. The laser pulse first forms a filament after approximately 199 cm with a peak intensity of about 0.8×10^{14} W cm^{-2} generating weak and well-resolved harmonics, visible before 210 cm in figure 4(b). The first intensity spike (A) is formed around 212 cm with a small peak intensity of about 0.9×10^{14} W cm^{-2}. The harmonics from this spike are also well resolved, as seen from the on-axis spectrum in figure 2(b), but have a spatial chirp that smears out the radially integrated spectrum (figure 4(b)). A second, much stronger spike (B) is formed around 219 cm, with a peak intensity above 2.5×10^{14} W cm^{-2}. This intensity occurs in an ultrashort sub-pulse in the trailing edge of the laser pulse, which generates a continuous spectrum both on-axis and off-axis. The cutoff energy of this spectrum

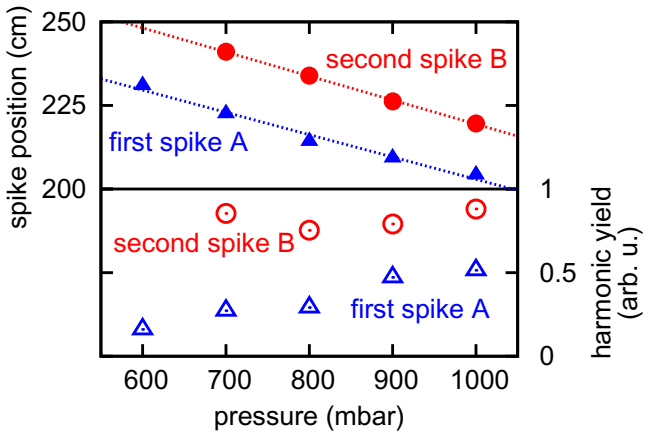

Figure 5. Control of the intensity spikes by variation of argon pressure. The upper graph shows the position of the intensity spikes with respect to the focusing optics by evaluating the location of maximum harmonic generation. The lower graph shows the maximum harmonic yield at that position.

is similar to that around 212 cm because of a strong blue-shift of the central frequency of the intense sub-pulse, see also [31, 32]. Just before the filament disperses, a third spike (C) is formed around 224 cm with an intensity that is high only on axis. Its contribution to the radially integrated harmonic yield is therefore minor. The agreement between the measured and calculated harmonic spectra at different positions in the filament is excellent, in particular in terms of the existence of and spacing between the intensity spikes, and in the highest harmonics generated. Moreover, the agreement is as well corroborated comparing the power spectrum of the spectrally broadened fundamental pulse at different propagation distances in the filament [45].

In the continuum region around 219 cm, the simulation predicts the occurrence of an IAP directly from filamentation after spectral filtering below order 16 with pulse energies similar to the experiment, shown in figure 4(c). The formation of the ∼500 as pulse is robust as seen from the relatively small change in shape over more than 1 cm of propagation. The time structure of the XUV light is sensitive to the initial laser CEP. For the case shown in figure 4(c), changing the laser CEP by $\pi/2$ gives rise to two to three attosecond pulses rather than one. This differs from the observations of the experimental single-shot measurements, in which we obtain a continuous harmonic spectrum for each laser shot of a different initial CEP. We note that in the calculations the CEP sensitivity is not caused by spatial averaging, and does not disappear by far-field spatial filtering.

6. Spike control

In our experiment, we can control the production of harmonics via the filament dynamics by changing the position, shape and relative amplitude of the intensity spikes. In figure 5, the harmonic yield and the position of the two regions in the filament are shown as a function of the argon pressure. Our data demonstrate the occurrence of intensity spikes over a very broad pressure range. While the harmonic yield from the first spike increases slowly with increasing pressure, the onset of the second spike appears suddenly at 700 mbar with a constant yield

at higher pressures. The top graph indicates that increasing pressure results in a shift of the spikes towards the focusing optics, caused by increased self-focusing due to higher nonlinear coefficients and shorter nonlinear length scales at higher pressure. This leads to an earlier start of the filament, which is confirmed by our calculations. The existence of the spikes is robust on a wide range of positive chirp values, spanning over 900 fs^2. In contrast, we have observed that the distance between the two spikes can change substantially when the chirp is varied. Furthermore, there are various possibilities for controlling the separation and the relative harmonic yield of the spikes via the spatiotemporal characteristics of the driving laser pulse. For example, by reducing the beam diameter by about 30% with an aperture before focusing, the relative harmonic yield of the second spike with respect to the yield of the first spike increases by more than a factor of 50. Among others, these parameters can be utilized for the precise control of emerging attosecond pulses with the possibility of switching between pulse trains or IAPs by selecting the position of generation within the filament.

7. Conclusion and outlook

In conclusion, we have shown that high-order harmonics can be generated and extracted directly from a filament. We attribute this to the formation of intensity spikes in the laser field at certain positions. One of these intensity spikes generates a continuous harmonic spectrum that appears to be independent of the initial laser CEP value and is preserved from shot to shot. We showed that our experimental findings are in excellent agreement with numerical results which attribute the continuum XUV spectrum to a near-single-cycle sub-pulse with the emergence of IAPs directly from the filament. Our results not only indicate a new and simple route to the production of IAPs from multicycle, commercially available laser systems, but also offer a new ultra-fast measurement tool for probing the rich, strong-field dynamics of femtosecond filamentation. Applying this filamentation probe in molecular gases may in turn become a new technique for investigating the molecular wave packet dynamics under the effect of an intense field [46].

Acknowledgments

This work was funded by Deutsche Forschungsgemeinschaft within the Cluster of Excellence QUEST, Centre for Quantum Engineering and Space-Time Research. MBG was supported by the National Science Foundation under grant number PHY-0449235 and by the PULSE Institute at Stanford University.

References

[1] Baker S, Robinson J S, Haworth C A, Teng H, Smith R A, Chirila C C, Lein M, Tisch J W G and Marangos J P 2006 Probing proton dynamics in molecules on an attosecond time scale *Science* **312** 424–7

[2] Li W, Zhou X, Lock R, Patchkovskii S, Stolow A, Kapteyn H C and Murnane M M 2008 Time-resolved dynamics in N_2O_4 probed using high harmonic generation *Science* **322** 1207–11

[3] Krausz F and Ivanov M 2009 Attosecond physics *Rev. Mod. Phys.* **81** 163–234

[4] L'Huillier A, Descamps D, Johansson A, Norin J, Mauritsson J and Wahlström C-G 2003 Applications of high-order harmonics *Eur. Phys. J.* D **26** 91–8

[5] Itatani J, Levesque J, Zeidler D, Niikura H, Pépin H, Kieffer J C, Corkum P B and Villeneuve D M 2004 Tomographic imaging of molecular orbitals *Nature* **432** 867–71

[6] Gohle C, Udem T, Herrmann M, Rauschenberger J, Holzwarth R, Schuessler H A, Krausz F and Hänsch T W 2005 A frequency comb in the extreme ultraviolet *Nature* **436** 234–7
[7] Hentschel M, Kienberger R, Spielmann Ch, Reider G A, Milosevic N, Brabec T, Corkum P, Heinzmann U, Drescher M and Krausz F 2001 Attosecond metrology *Nature* **414** 509–13
[8] Agostini P and DiMauro L F 2004 The physics of attosecond light pulses *Rep. Prog. Phys.* **67** 813–55
[9] Goulielmakis E *et al* 2008 Single-cycle nonlinear optics *Science* **320** 1614
[10] Sola I J *et al* 2006 Controlling attosecond electron dynamics by phase-stabilized polarization gating *Nat. Phys.* **2** 319–22
[11] Tzallas P, Skantzakis E, Kalpouzos C, Benis E P, Tsakiris G D and Charalambidis D 2007 Generation of intense continuum extreme-ultraviolet radiation by many-cycle laser fields *Nat. Phys.* **3** 846–50
[12] Mashiko H, Gilbertson S, Li C, Khan S D, Shakya M M, Moon E and Chang Z 2008 Double optical gating of high-order harmonic generation with carrier-envelope phase stabilized lasers *Phys. Rev. Lett.* **100** 103906
[13] Sansone G *et al* 2006 Isolated single-cycle attosecond pulses *Science* **314** 443–6
[14] Altucci C, Esposito R, Tosa V and Velotta R 2008 Single isolated attosecond pulse from multicycle lasers *Opt. Lett.* **33** 2943–5
[15] Nisoli M, de Silvestri S, Svelto O, Szipöcs R, Ferencz K, Spielmann Ch, Sartania S and Krausz F 1997 Compression of high-energy laser pulses below 5 fs *Opt. Lett.* **22** 522–4
[16] Wagner N L, Gibson E A, Popmintchev T, Christov I P, Murnane M M and Kapteyn H C 2004 Self-compression of ultrashort pulses through ionization-induced spatiotemporal reshaping *Phys. Rev. Lett.* **93** 173902
[17] Sandhu A S, Gagnon E, Paul A, Thomann I, Lytle A, Keep T, Murnane M M, Kapteyn H C and Christov I P 2006 Generation of sub-optical-cycle, carrier-envelope-phase-insensitive, extreme-UV pulses via nonlinear stabilization in a waveguide *Phys. Rev.* A **74** 061803
[18] Thomann I, Bahabad A, Liu X, Trebino R, Murnane M M and Kapteyn H C 2009 Characterizing isolated attosecond pulses from hollow-core waveguides using multi-cycle driving pulses *Opt. Express* **17** 4611
[19] Uiberacker M *et al* 2007 Attosecond real-time observation of electron tunnelling in atoms *Nature* **446** 627
[20] Zhang X, Lytle A, Popmintchev T, Paul A, Wagner N, Murnane M and Kapteyn H 2005 Phase matching, quasi-phase matching and pulse compression in a single waveguide for enhanced high-harmonic generation *Opt. Lett.* **30** 1971–3
[21] Arpin P, Popmintchev T, Wagner N L, Lytle A L, Cohen O, Kapteyn H C and Murnane M M 2009 Enhanced high harmonic generation from multiply ionized argon above 500 eV through laser pulse self-compression *Phys. Rev. Lett.* **103** 143901
[22] Takahashi E, Nabekawa Y and Midorikawa K 2002 Generation of 10-μJ coherent extreme-ultraviolet light by use of high-order harmonics *Opt. Lett.* **27** 1920
[23] Tosa V, Takahashi E, Nabekawa Y and Midorikawa K 2003 Generation of high-order harmonics in a self-guided beam *Phys. Rev.* A **67** 063817
[24] Hauri C P, Kornelis W, Helbing F W, Couairon A, Mysyrowicz A, Biegert J and Keller U 2004 Generation of intense carrier–envelope phase-locked few-cycle laser pulses through filamentation *Appl. Phys.* B **79** 673–7
[25] Couairon A, Biegert J, Hauri C P, Kornelis W, Helbing F W, Keller U and Mysyrowicz A 2006 Self-compression of ultra-short laser pulses down to one optical cycle by filamentation *J. Mod. Opt.* **53** 75
[26] Steingrube D S, Schulz E, Binhammer T, Vockerodt T, Morgner U and Kovačev M 2009 Generation of high-order harmonics with ultra-short pulses from filamentation *Opt. Express* **17** 16177–82
[27] Couairon A and Mysyrowicz A 2007 Femtosecond filamentation in transparent media *Phys. Rep.* **441** 47–189
[28] Zaïr A, Guandalini A, Schapper F, Holler M, Biegert J, Gallmann L, Couairon A, Franco M, Mysyrowicz A and Keller U 2007 Spatio-temporal characterization of few-cycle pulses obtained by filamentation *Opt. Express* **15** 5394–405
[29] Kolesik M and Moloney J V 2004 Self-healing femtosecond light filaments *Opt. Lett.* **29** 590–2
[30] Dubietis A, Gaižauskas E, Tamošauskas G and Di Trapani P 2004 Light filaments without self-channeling *Phys. Rev. Lett.* **92** 253903

[31] Chakraborty H S, Gaarde M B and Couairon A 2006 Single attosecond pulses from high harmonics driven by self-compressed filaments *Opt. Lett.* **31** 3662–4
[32] Gaarde M B and Couairon A 2009 Intensity spikes in laser filamentation: diagnostics and application *Phys. Rev. Lett.* **103** 043901
[33] Papadogiannis N A, Kalpouzos C, Goulielmakis E, Nersisyan G, Charalambidis D, Augé F, Weihe F and Balcou Ph 2001 Kilohertz extreme-ultraviolet light source based on femtosecond high-order harmonic generation from noble gases *Appl. Phys.* B **73** 687–92
[34] Steingrube D S, Vockerodt T, Schulz E, Morgner U and Kovačev M 2009 Phase-matching of high-order harmonics in a semi-infinite gas cell *Phys. Rev.* A **80** 043819
[35] Lange H R, Chiron A, Ripoche J-F, Mysyrowicz A, Breger P and Agostini P 1998 High-order harmonic generation and quasiphase matching in xenon using self-guided femtosecond pulses *Phys. Rev. Lett.* **81** 1611
[36] Painter J C, Adams M, Brimhall N, Christensen E, Giraud G, Powers N, Turner M, Ware M and Peatross J 2006 Direct observation of laser filamentation in high-order harmonic generation *Opt. Lett.* **31** 3471
[37] Gaarde M B, Tate J L and Schafer K J 2008 Macroscopic aspects of attosecond pulse generation *J. Phys. B: At. Mol. Opt. Phys.* **41** 132001
[38] Ilkov F A, Decker J E and Chin S L 1992 Ionization of atoms in the tunnelling regime with experimental evidence using Hg atoms *J. Phys. B: At. Mol. Opt. Phys.* **25** 4005
[39] Lewenstein M, Balcou Ph, Ivanov M Yu, L'Huillier A and Corkum P B 1994 Theory of high-harmonic generation by low-frequency laser fields *Phys. Rev.* A **49** 2117–32
[40] Henke B L, Gullikson E M and Davis J C 1993 X-ray interactions: photoabsorption, scattering, transmission and reflection at $E = 50$–30000 eV, $Z = 1$–92 *At. Data Nucl. Data Tables* **54** 181
[41] L'Huillier A, Li X F and Lompre L A 1990 Propagation effects in high-order harmonic generation in rare gases *J. Opt. Soc. Am.* B **7** 527
[42] Krause J L, Schafer K J and Kulander K C 1992 High-order harmonic generation from atoms and ions in the high intensity regime *Phys. Rev. Lett.* **68** 3535–8
[43] Faccio D, Averchi A, Lotti A, Di Trapani P, Couairon A, Papazoglou D and Tzortzakis S 2008 Ultrashort laser pulse filamentation from spontaneous X wave formation in air *Opt. Express* **16** 1565–70
[44] Faccio D, Lotti A, Matijosius A, Bragheri F, Degiorgio V, Couairon A and Di Trapani P 2009 Experimental energy-density flux characterization of ultrashort laser pulse filaments *Opt. Express* **17** 8193–200
[45] Schulz E, Steingrube D S, Binhammer T, Gaarde M B, Couairon A, Morgner U and Kovačev M 2011 Tracking spectral shapes and temporal dynamics along a femtosecond filament (in preparation)
[46] Odhner J H, Romanov D A and Levis R J 2009 Rovibrational wave-packet dispersion during femtosecond laser filamentation in air *Phys. Rev. Lett.* **103** 075005